ELSEVIER

Ocean Modelling 3 (2001) 95–108

Ocean Modelling

www.elsevier.com/locate/omodol

Realistic representation of the surface freshwater flux in an ice–ocean general circulation model

B. Tartinville *, J.-M. Campin [1], T. Fichefet, H. Goosse

Institut d'Astronomie et de Géophysique G. Lemaître, Université Catholique de Louvain, 2 Chemin du Cyclotron, B-1348 Louvain-la-Neuve, Belgium

Received 6 November 2000; received in revised form 22 January 2001; accepted 22 January 2001

Abstract

Ocean general circulation models usually use an equivalent salt-flux in order to represent the freshwater surface inflow/outflow. This unphysical approach has numerous shortcomings, especially for climate studies. A more physical representation has been originally proposed by R.X. Huang [Journal of Physical Oceanography 23 (1993) 2428–2446] for ocean models. It consists in taking into account the vertical velocity at the sea surface. Here this formulation is introduced in a coupled ice–ocean general circulation model designed for climate studies. The treatment of the ice–ocean exchanges needs special care in order to conserve salt and freshwater masses, and to correctly represent the physics involved. This formulation allows to simulate the Goldsbrough–Stommel circulation and the meridional pathway of the freshwater at the ocean surface. Furthermore, the meridional freshwater transport diagnosed using such an approach is more directly comparable to the atmospheric water-vapor transport. Nevertheless, it produces only small changes in the ocean general circulation.

Keywords: Ocean modeling; Freshwater; Flux

1. Introduction

As it is an important element of the hydrological cycle, the freshwater flux at the sea surface has an impact on the climate system (Webster, 1994). In the past, sudden freshwater discharges to the ocean are known to have greatly perturbed the climate (e.g., Bond et al., 1992; Manabe and

* Corresponding author. Tel.: +33-10-47-32-98; fax.: +33-10-47-47-22.
E-mail address: tartin@astr.ucl.ac.be (B. Tartinville).
[1] Present Address: Department of Earth, Atmospheric, and Planetary Science, Massachusetts Institute of Technology, Cambridge, Massachusetts.

1463-5003/01/$ - see front matter
PII: S1463-5003(01)00003-8

Stouffer, 1995; Barber et al., 1999). Nowadays, among the major oceanic basins, the Atlantic is an evaporative one, whereas the Pacific receives an excess of about 0.9×10^6 m^3 s^{-1} of freshwater from the atmosphere (Baumgartner and Reichel, 1975). As a consequence, the present oceanic circulation transports freshwater from the Pacific to the Atlantic. This flow is counterbalanced by an atmospheric water-vapor transport. Meridional atmospheric water-vapor transport also occurs from low to high latitudes. Furthermore, as it has an impact on the density of the water masses and on the stability of the water column, the freshwater flux at the sea surface plays a significant role in the formation of North Atlantic deep water (NADW) and thus in the thermohaline circulation (e.g., Broecker et al., 1990; Cai, 1996). The possible impact of the freshwater input on the climate of the next centuries has been widely discussed (e.g., Stocker and Schmittner, 1997). A potential greenhouse-gas-induced increase of precipitation in the Atlantic could induce a less pronounced NADW formation and hence a reduction of the northward oceanic heat flux which is responsible for the mild winter climate over Western Europe.

Despite its important role, little attention has been paid to the treatment of the surface freshwater flux in ocean general circulation models. Because, salt exchanges between the atmosphere and the ocean are rather weak and land–sea exchanges occur on geological time scales, the mass of salt present within the ocean should remain almost constant on climatic time scales. Therefore, if the freshwater forcing is balanced, the mean salinity should remain constant. Since the pioneering rigid-lid model of Bryan (1969), the freshwater flux at the sea surface has been usually parameterised as an equivalent salt-flux: salt is removed/introduced at the sea surface in order to take into account the dilution effect. Though unphysical, this representation has been maintained in more recent models. The shortcomings of this classical approach have been discussed by Huang (1993) and are summarised here. So as to represent the dilution effect, one should use a local salinity in order to convert freshwater flux into salt-flux. But, this induces a positive/negative feedback in regions of high/low salinity which leads to a continuous, although weak, increase in global salinity (see details in Huang, 1993). Using a fixed mean sea-surface salinity overcomes this problem but does not accurately represent the local dilution effect. Furthermore, it does not take into account a potential drift in sea-surface salinity, which is more than likely in climate-change experiments, and it is thus difficult to define an adequate reference salinity. As an example, since the sea level was lower than today by about 120 m during the Last Glacial Maximum (Bard et al., 1996), the mean ocean salinity was about 1 psu higher during this period than today.

As an improvement, a more physical representation of this atmospheric flux could be introduced by taking into account the vertical velocity at the air–sea interface (Huang, 1993; Beron-Vera et al., 1999). This new surface boundary condition suppresses pitfalls of the classical approach. It allows a better representation of the freshwater transport within an ocean general circulation model and of the hydrological cycle within a coupled ocean–atmosphere model. The impact of the dilution on anthropogenic or natural tracers, which are usually used in ocean general circulation models (e.g., England, 1995; Goosse et al., 1999), is naturally incorporated in the new formulation without any additional unphysical terms. Furthermore, the inflow of geochemical tracers at river mouths is more simply introduced. This formulation has been tested, together with other surface boundary conditions, within a rigid-lid model of the Atlantic Ocean by Wadley et al. (1996). According to this study, at short time scales, it produces a much more realistic pattern of the sea-surface salinity, temperature and current than the equivalent salt-flux

method. It has also been tested within an ocean general circulation model on time scales from season to decades by Roullet and Madec (2000). They conclude that the formulation has an impact on the salinity distribution near river mouths and also in the ocean interior. However, both models have not been integrated for a sufficient time period in order to produce a significant change in the thermohaline circulation. A longer experiment is therefore required in order to investigate the effect of this formulation on the thermohaline circulation and on the properties of deep waters. Because sea ice plays an important role on the water storage and freshwater transport at high latitudes, it seems necessary to implement and test this formulation within a coupled ice–ocean general circulation model. To our knowledge, this has not yet been done within such a model or within a more complex ice–ocean–atmosphere model.

Two experiments are carried out: the first one is conducted with the equivalent salt-flux parameterisation, while the second one is performed with the realistic freshwater flux formulation. In the next section, the two formulations are described. As the realistic freshwater flux approach is included for the first time in an ice–ocean model, we will put emphasis on the description of ice–ocean salt and mass exchanges. Model results and adequate diagnostics are presented in the following sections.

2. Model description and surface boundary conditions

The model used in the present study is a three-dimensional, free-surface, coupled sea ice–ocean general circulation model described in Goosse et al. (1999). It has a resolution of $3° \times 3°$ on the horizontal and 20 uneven vertical levels. In order to avoid a singularity at the North Pole, a rotated grid is used for the Arctic and the North Atlantic Oceans, whereas a longitude–latitude grid is used for the remaining part of the ocean. The Pacific and Arctic Oceans are connected through Bering Strait where the flow is calculated assuming a geostrophic control of the transport. A turbulent closure scheme, which solves one differential equation for the turbulent kinetic energy, is used in order to represent the vertical mixing in the upper ocean. The sea-ice component is a thermodynamic–dynamic model with viscous-plastic rheology.

The model is forced by surface heat and momentum fluxes derived from monthly mean climatological fields of surface air temperature, air relative humidity, cloud cover, wind speed, and wind stress. Details on those climatological forcing fields can be found in Goosse et al. (1999). The freshwater forcing requires a special attention. Evaporation, E, is derived from the latent heat-flux calculation. The freshwater inflow is derived from the monthly precipitation fields of Xie and Arkin (1996) and from runoff data of Baumgartner and Reichel (1975) and Grabs et al. (1996). Because precipitation data have a great uncertainty, we allow the addition of an extra freshwater inflow which is calculated as described below. A 1000-year spin-up simulation is first carried out with the same forcing fields and with an additional restoring term towards Levitus (1982) sea-surface salinities – time constant is two months for the 10-m-thick surface grid box. The additional freshwater inflow necessary to maintain realistic sea-surface salinities is diagnosed from this spin-up experiment. It is then added to the climatological precipitation and runoff forcing fields. Since sea-surface salinities from Levitus are known to be unrealistic below sea ice, this corrective term is not used in the Arctic Ocean and southward of 70°S. This method, quite similar to the one proposed by Gent et al. (1998), allows to have the same freshwater input in all our experiments

and to maintain realistic sea-surface salinities without using a restoring term towards observed values. The latter would damp the differences between our experiments. This method produces a freshwater inflow field, P, which encompasses precipitation, runoff, and the corrective term, depicted in Fig. 1. This field can be compared to the one displayed in Fig. 19 of Gent et al. (1998). It is negative in certain locations, although values are close to zero. Two 200-year numerical experiments are then carried out starting from the results of the 1000-year spin-up experiment. The sole difference lies in the surface boundary conditions: the equivalent salt-flux approach or the realistic freshwater flux approach.

The kinematic equation represents the upper surface boundary condition. The positive downward volume flux at the sea surface, F_f, is included in this equation following

$$\frac{\partial \eta}{\partial t} = -u(\eta)\frac{\partial \eta}{\partial x} - v(\eta)\frac{\partial \eta}{\partial y} + w(\eta) + F_f, \tag{1}$$

where η denotes the sea-surface elevation relatively to a fixed reference vertical level ($z = 0$), x and y are the zonal and meridional coordinates, u and v are the zonal and meridional velocity components, respectively, and w is the vertical velocity component, positive upwards. Assuming that the two first terms in the right-hand side of (1) are negligible, and since the model used in this study has fixed vertical levels (the upper limit of the model computational domain is located at $z = 0$), the boundary condition (1) reduced to

$$\frac{\partial \eta}{\partial t} = w(0) + F_f. \tag{2}$$

Ocean tracers are transported following the classical advection/diffusion equation. Surface fluxes (F_s for salinity and F_t for temperature) are specified at the top of the ocean according to atmosphere-ocean and ice–ocean exchanges.

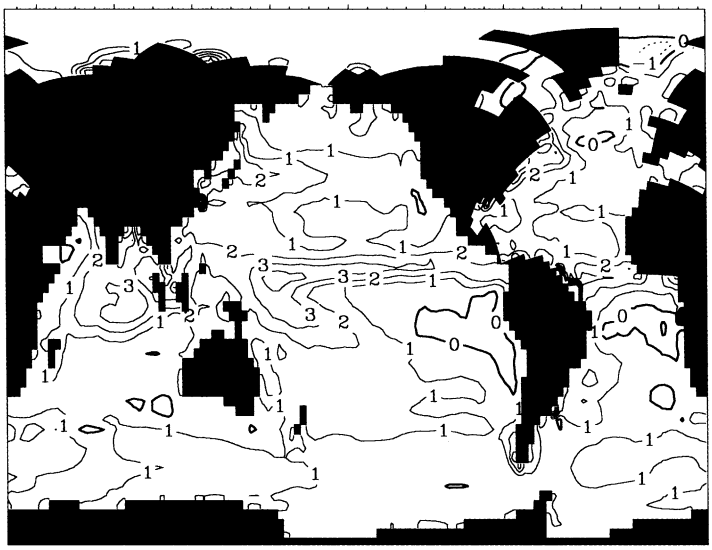

Fig. 1. The annual mean freshwater inflow (m yr^{-1}) derived from climatological fields and from the spin-up experiment. Contour interval is 1 m yr^{-1}.

In comparison to direct air–sea freshwater exchanges due to precipitation and evaporation, the treatment of the flux between sea ice and the ocean requires a special attention. Indeed, the exchanges of freshwater between sea ice and the ocean during melting and freezing do not contribute to a modification of the pressure field in the ocean at a reference level. Furthermore, ice acts as a blanket that delays the dilution effect due to snow precipitation until ice has melted away.

2.1. Equivalent salt-flux experiment

For the equivalent salt-flux approach, the volume flux at the upper boundary is nil. In order to accurately represent the dilution effect due the freshwater inflow, an equivalent salt-flux is applied at the sea surface. Salt and freshwater exchanges at the ice–ocean interface are included in F_s as described in Fichefet and Morales Maqueda (1997). Then, the inflows at the sea surface read

$$F_f = 0, \tag{3a}$$

$$F_s = \frac{1}{\Delta z_s}\left[S_{ref}(E-P) + \frac{S_{ref}}{\rho_0}\left(\frac{\partial m_s}{\partial t}\right)_{abl} + \frac{(S_{ref}-S_{ice})}{\rho_0}\left(\frac{\partial m_i}{\partial t}\right)_{acc,abl} + \frac{(S_{ref}-S_{ice})}{\rho_0}\left(\frac{\partial m_s}{\partial t}+\frac{\partial m_i}{\partial t}\right)_{si} + \frac{S_{ice}}{\rho_0}\left(\frac{\partial m_s}{\partial t}\right)_{si}\right], \tag{3b}$$

where S_{ref} is a reference sea-surface salinity ($S_{ref} = 34.7$ psu), and S_{ice} is the sea-ice salinity ($S_{ice} = 4$ psu). ρ_0 is a reference ocean density and Δz_s is the thickness of the upper oceanic grid cell ($\Delta z_s = 10$ m). m_s and m_i are the masses of snow and ice per unit area, respectively. The first term on the right-hand side of (3b) represents the dilution effect due to evaporation, precipitation, and runoff. The second one simulates the freshwater flux to the ocean due to snow melting (labeled abl). The third one is associated with ice melting/formation (labeled abl and acc). The fourth and the fifth ones come from the snow-ice formation (labeled si). When the load of snow is large enough to depress the lower boundary of the snow layer under the water level, seawater is assumed to infiltrate the entirety of the submerged snow and to freeze there, forming a snow-ice cap. The fourth term represents the salt rejection that occurs because of the freezing of the seawater. The fifth term corresponds to the salt-flux needed to bring the fresh snow to the sea-ice salinity (4 psu) during its transformation into snow ice. The 200-year control experiment performed with this boundary condition is hereafter referred to as ESF.

2.2. Realistic freshwater flux experiment

Another approach is to introduce the freshwater flux in a more realistic way. Without sea ice, the freshwater inflow is only due to the air–sea exchanges and runoff. One can simply write $F_f = P - E$ and $F_s = 0$ (Huang, 1993). However, correctly taking into account the exchanges between sea ice and the ocean requires great care. For instance, when sea ice is formed, the brine released is more likely to be considered as a salt-flux rather than a freshwater flux. It should be noted also that the annual net ice formation/melting is of the order of the sea-surface displacement (1 m).

To distinguish between salt-flux and freshwater flux, the following two rules are adopted. First, if liquid or solid water is added to or extracted from the ice–ocean system (e.g., through precipitation or evaporation), then it is introduced as a freshwater flux. This is a common approach applied in ocean models (Huang, 1993; Wadley et al., 1996; Roullet and Madec, 2000). Second, if surface process affects ocean salinity without a net gain or loss of water for the ice–ocean system (e.g., through ice melting or freezing) this internal exchange is transformed into an equivalent salt-flux that is applied to the ocean. This principle ensures that mass exchange (i.e., $P - E$) does contribute to the variation of the pressure field at a reference level, whereas freshwater flux associated with ice melting and freezing does not. In this approach, sea ice acts as a negative reservoir of salt inside the ice–ocean system. As ice is formed, salt is released into the ocean. As ice melts, salt is taken out of the ocean.

Furthermore, because snow falling on the ice pack has no immediate effect on the seawater salinity below ice, this precipitation is incorporated into the freshwater flux towards the ocean not immediately but later: as soon as snow melts or is transformed into snow ice. At this time, only freshwater is added when snow melts, whereas when it is transformed into snow ice, both freshwater and salt are incorporated into the ocean simultaneously. This is necessary in order to account for both snow precipitation and ice formation. The shortcoming of this approach is that the effect of snow precipitation over the ice pack on the ocean pressure field is delayed until snow melts or is transformed into snow ice.

The net heat flux at the ocean surface is usually derived from the latent, sensible, solar, and long-wave fluxes (the sum of those term is here denoted Q). However, an additional flux must be added in order to represent heat transported with the freshwater inflow. It is here assumed that a freshwater parcel entering or exiting the ocean has the same temperature as the surface ocean, T_s. Therefore, the surface fluxes read

$$F_f = P - E - \frac{1}{\rho_0}\left(\frac{\partial m_s}{\partial t}\right)_{abl,si}, \tag{4a}$$

$$F_s = \frac{(S_{ref} - S_{ice})}{\rho_0 \Delta z_s}\left(\frac{\partial m_i}{\partial t}\right)_{acc,abl,si}, \tag{4b}$$

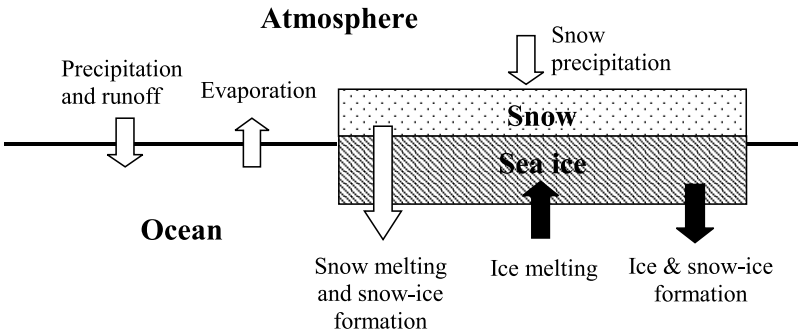

Fig. 2. Schematic representation of the salt (black arrows) and freshwater (white arrows) fluxes used in RFF.

$$F_t = Q + \frac{T_s}{\Delta z_s} F_f. \tag{4c}$$

Freshwater and salt-fluxes used in this experiment are sketched in Fig. 2. Experiment RFF includes this new formulation of the freshwater flux at the air–sea interface. It should be noted that numerous model refinements could be introduced in order to perfectly take into account the effect

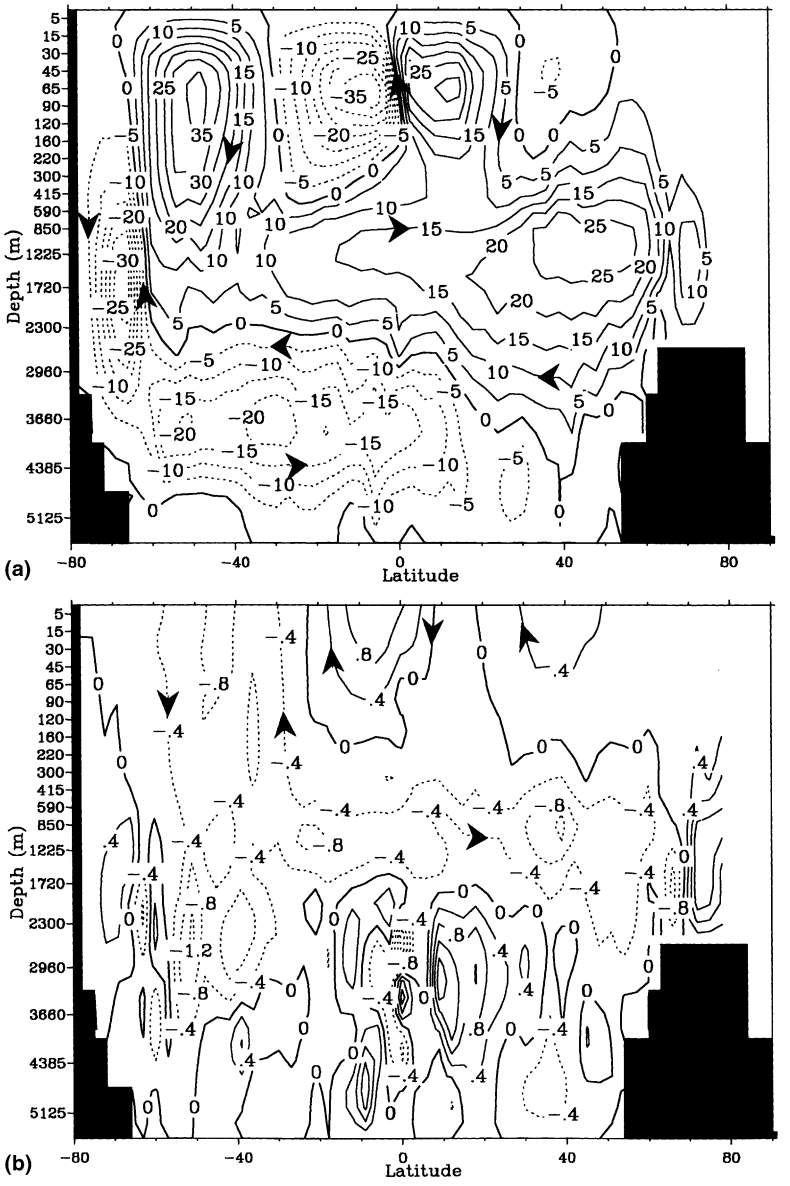

Fig. 3. (a) Global meridional overturning stream-function (Sv) as calculated by the model in ESF. Contour interval is 5 Sv. (b) Differences in global meridional overturning stream-function between RFF and ESF (Sv). Contour interval is 0.4 Sv.

of the surface freshwater forcing, including varying level thickness. Though it does not strictly conserve salt, our model is a free-surface with fixed level thickness, which appears to be the best compromise in order to introduce the freshwater flux in a realistic way in climate models (Roullet and Madec, 2000).

3. Model results

Results presented here are averaged values over the last 10 years of our two experiments. Fig. 3(a) depicts the global overturning stream-function as calculated by the model in ESF. It produces a reasonable thermohaline circulation with an anti-clockwise circulation cell due to the formation of NADW and a bottom clockwise circulation cell caused by the formation of Antarctic bottom water (AABW). In the model, NADW formation mainly occurs south of the Denmark Strait. About 21 Sv ($1\ \mathrm{Sv} = 10^6\ \mathrm{m}^3\ \mathrm{s}^{-1}$) of NADW is exported out of the Atlantic Ocean at 30°S, which is in the higher side of the range of observational estimates (McDonald and Wunsch, 1996). The deepest part of the ocean is filled with relatively cold AABW, which is formed along Antarctica and partly penetrates into the Atlantic Ocean at a rate of about 4.5 Sv. For the realistic freshwater flux approach, the meridional circulation is still non-divergent in the ocean interior, and the meridional stream-function could be calculated in a classical manner, specifying a zero value at the ocean bottom. From the differences in global meridional stream-function between our two experiments (Fig. 3(b)), it appears that the realistic freshwater flux boundary condition does not drastically affect the thermohaline circulation. For instance, the formation rate of NADW is only reduced by 0.1 Sv. Due to a concomitant weakening of the AABW flow towards the Atlantic, the export of NADW out of this ocean is enhanced by about 0.3 Sv. Furthermore, the export of AABW towards the Pacific and Indian Oceans is slightly enhanced in experiment RFF. This leads to a global, although weak, decrease of the meridional overturning stream-function at a depth of about 1000 m, as depicted in Fig. 3(b).

In contrast with experiment ESF, experiment RFF should include what is called the Goldsbrough–Stommel circulation. It is made of a cyclonic gyre in the subtropics and of an anticyclonic gyre in the subpolar regions, which are driven by the vertical pumping induced by the evaporation and precipitation (Stommel, 1984). As the intensity of this circulation is much weaker than the intensity of the wind-driven gyres, this circulation can only be identified by looking at the difference between the two experiments. In the Pacific Ocean, the difference in the barotropic stream-function between our two simulations corresponds mainly to the Goldsbrough–Stommel circulation (Fig. 4). The intensity of the gyres (less than 1 Sv) is in accordance with theoretical considerations. For the Indian Ocean, the difference also corresponds to the Goldsbrough–Stommel circulation. However, changes in the barotropic circulation are more important in the Atlantic Ocean (of the order of 2 Sv at maximum) and do not perfectly match this circulation pattern. This is possibly due to changes in the regions of deep-water formation and to the weak changes in the thermohaline circulation. In addition to this classical barotropic circulation, the difference between experiments RFF and ESF provides a new insight into the freshwater-induced circulation (Fig. 3(b)). Though discrepancies in the meridional transport are rather small, it clearly depicts the net freshwater inflow/outflow at the ocean surface and the path of this freshwater mainly in the upper part of the ocean. There is a net loss of freshwater in the subtropics and

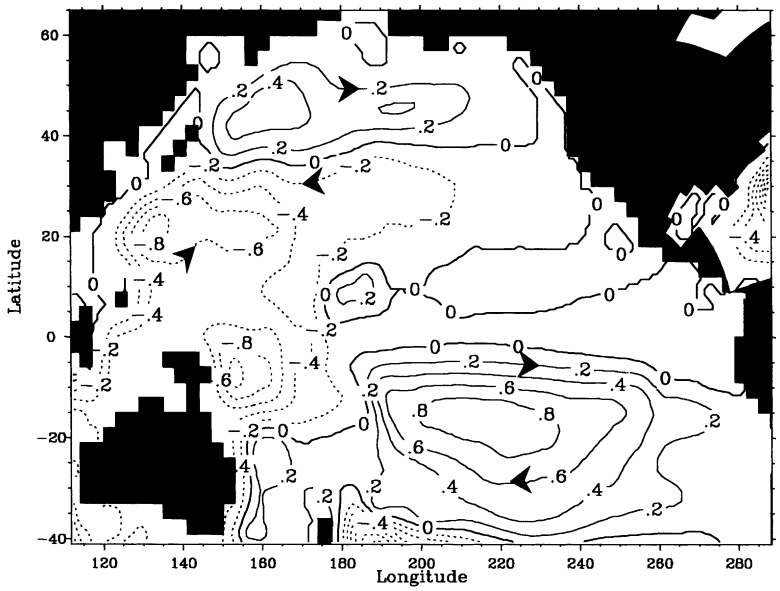

Fig. 4. Differences in barotropic stream-function between RFF and ESF (Sv) for the Pacific Ocean. Contour interval is 0.2 Sv.

a net gain at the equator and at higher latitudes. This is balanced by a freshwater transport within unclosed surface cells, the intensity of which is equal to the net zonally averaged freshwater inflow.

The use of a non-zero vertical velocity at the ocean surface in experiment RFF induces a vertical pumping in regions of net evaporation. Although it is much weaker than the Ekman pumping, it induces an additional vertical displacement of the pycnocline. This leads to a zonal mean decrease in temperature and salinity at the base of the pycnocline of 0.1°C and 0.01 psu, respectively.

The differences in the sea-surface salinity between our two experiments are significant at the river mouths in shallow areas (Fig. 5). At those places the exchange of freshwaters coming from the rivers and open ocean waters is more intense in RFF than in ESF. This induces the observed increase in sea-surface salinity in the Bay of Bengal, the North Sea, the Gulf of Guinea and the Yellow Sea. In the Arctic Ocean, due to slow exchanges with other basins and to the important local river freshwater discharges, the difference in sea-surface salinity between our experiments is also pronounced. In other parts of the ocean, in particular around Antarctica, differences are rather small. Furthermore, as the Atlantic is a net evaporative basin, its surface salinity should be greater than the global reference salinity. Indeed, the Atlantic mean sea-surface salinity in experiment ESF is 35.84 psu (to be compared to 35.79 psu in Levitus, 1982); i.e., 1.14 psu larger than S_{ref}. Since the representation of the dilution effect uses the latter value instead of a local salinity in this experiment, this induces an enhanced salt-flux towards this basin. Therefore, though difference is small, the mean Atlantic surface salinity in experiment ESF is 0.025 psu greater than in experiment RFF.

In the classical approach (experiment ESF), the wind-driven gyres and the thermohaline circulation transport salt from regions of net evaporation towards regions of net precipitation. No

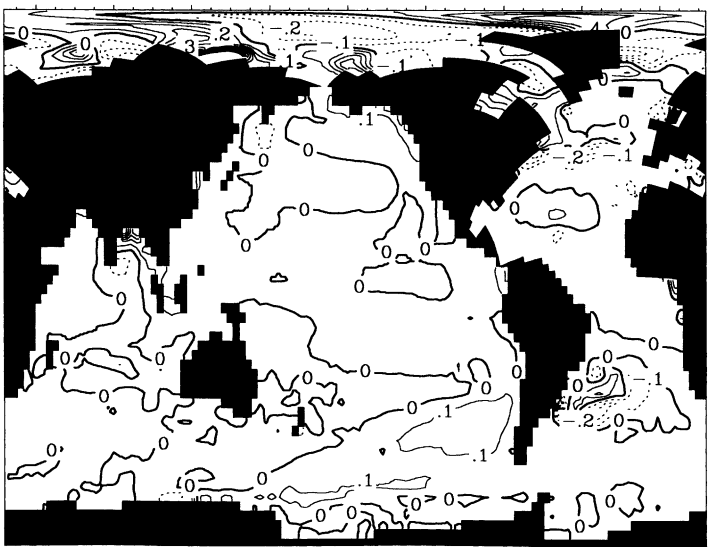

Fig. 5. Differences in sea-surface salinity between RFF and ESF (psu). Contour interval is 0.1 psu.

freshwater is transported in this experiment. The classical way to diagnose the northward freshwater transport, NWT_{ESF}, in ocean general circulation models is to calculate the ratio of the negative salt transport to the reference salinity, S_{ref}. It reads

$$NWT_{\mathrm{ESF}} = -\frac{\overline{vs}}{S_{\mathrm{ref}}}, \tag{5}$$

where v is the meridional oceanic velocity (positive northwards) and s is the oceanic salinity. The overbar denotes an integration over a zonal section.

This calculation is no longer valid for the realistic freshwater flux surface boundary condition. For RFF, the freshwater transport, NWT_{RFF}, is simply diagnosed from the integration of the meridional oceanic velocity:

$$NWT_{\mathrm{RFF}} = \bar{v}. \tag{6}$$

Since there is no meridional oceanic transport in ESF, NWT_{RFF} could be diagnosed from Fig. 3(b) as the opposite of the meridional stream-function at the ocean surface. Under the realistic assumption that the mass of salt is negligible in comparison to the mass of "pure water" present in a reference oceanic volume, (6) is similar to the equation proposed by Wijffels et al. (1992). This equation has the great advantage that it does not depend on a reference salinity which should vary on climatic time scales.

The northward freshwater transports as calculated from Eqs. (5) and (6) are depicted in Fig. 6 together with estimates from Wijffels et al. (1992) and da Silva et al. (1994). The two model curves are quite close to each other, except at high latitudes in both hemispheres, where small differences are noticeable. South of 60°S, ESF produces a southward freshwater transport, whereas it is northward in RFF. This difference is related to the ice–ocean salt exchanges. In both formulations, salt is released into the ocean in regions of ice growth, whereas salt is extracted from the ocean in regions of ice melting. In the Southern Hemisphere, as ice formation primarily occurs on

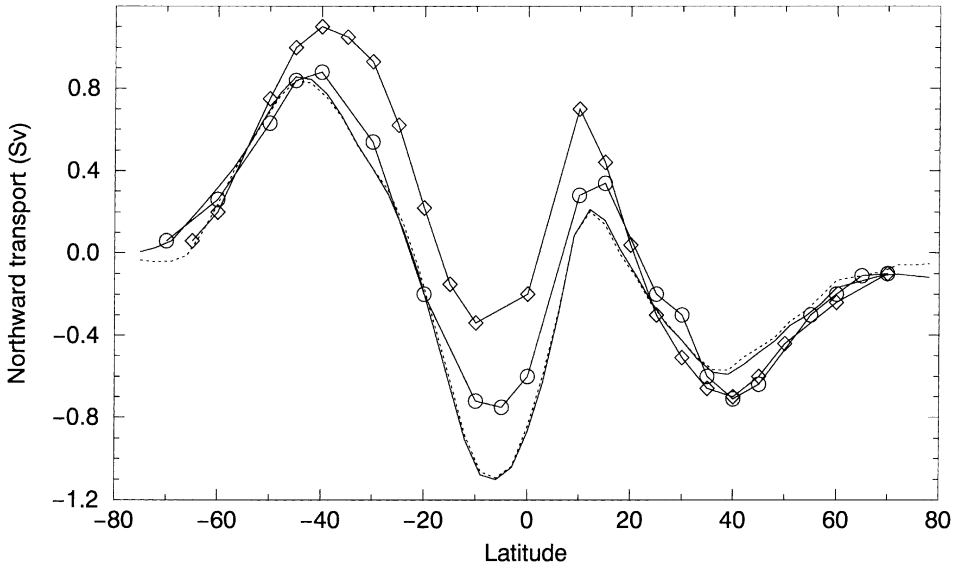

Fig. 6. Northward freshwater transports (Sv) derived from ESF (dotted line), RFF (thin line), Wijffels et al. (1992) (thin line with circles), and da Silva et al. (1994) (thin line with diamonds).

continental shelves and ice is advected northwards where it melts, the modeled ice drift transports salt southwards. In order to compensate for this net flux, the ocean must transport salt northwards. It must be stressed that the calculation of NWT_{ESF}, which derives from the oceanic salt transport, includes this additional southward freshwater transport at high latitudes, whereas it is not included in NWT_{RFF}, which does not take into account salt exchanges due to ice melting and freezing. From a previous estimate of Goosse et al. (1997), using an earlier version of the same ocean–sea–ice model, the net ice-formation rate over the 2.8×10^6 km^2 continental shelves around Antarctica is equivalent to a negative freshwater flux of 1.9 m per year. This corresponds to a southward freshwater transport of 0.17 Sv onto the shelves. This value is rather similar to the maximum difference between our two curves in the Southern Ocean (0.15 Sv). For the same reason, the two calculated transports are different at high northern latitudes. The difference between the two curves at 78°N (i.e., at the latitude of the Fram Strait) is about 0.07 Sv. This is close to the modeled sea-ice export through this strait (0.06 Sv), which is within the range of current estimates (Kwok and Rothrock, 1999).

Since NWT_{RFF} does not take into account the equivalent salt transport from the regions of ice formation towards regions of ice melting, NWT_{RFF} corresponds to the freshwater transport of the ice–ocean system, and is therefore more directly comparable to the atmospheric water-vapor transport deduced from observations or modeling studies. It should be noted that, though weak, the freshwater transport associated with the drift of the snow layer present at the top of the ice cap is not included in NWT_{RFF}.

The northward freshwater flux derived from both experiments is rather similar to the one proposed by Wijffels et al. (1992). A noticeable difference occurs south of the equator, where the simulated southward flux is too intense. This comes from a too strong tropical evaporation in the model Southern Hemisphere in comparison to the data used in Wijffels et al. (1992). Nevertheless,

the difference between the model experiments and this estimate is much smaller than the difference between the two independent estimates. Furthermore, at 30°S in the model, the Atlantic Ocean receives freshwater at a rate of about 0.28 Sv. This value is comparable to other estimates (e.g., McDonald, 1993).

4. Summary and conclusions

An equivalent salt-flux approach is usually used in order to represent the surface freshwater inflow/outflow in ocean general circulation models. So as to solve the problems due to this approach, a new formulation of the freshwater inflow at the ocean surface, initially proposed by Huang (1993), has been here introduced in a coupled ocean–sea–ice general circulation model. A special attention was devoted to salt and freshwater exchanges at the ice–ocean interface. To test the effect of this new formulation, two 200-year numerical experiments have been carried out. The equivalent salt-flux approach is used in the first one, while the more physical freshwater flux approach is used in the second one. It appears that the differences between the two simulations are rather small. None the less, the Goldsbrough–Stommel circulation and the pathway of the freshwater at the ocean surface can be diagnosed clearly from the difference between the two experiments.

The calculation of the meridional freshwater transport is simpler in the new formulation and it does not drastically depend on an arbitrary reference surface salinity. Furthermore, since it does not include the meridional salt transport due to sea-ice formation/melting, the meridional freshwater transport derived from the new formulation appears to be more directly comparable with atmospheric water-vapor transport.

Numerical studies have demonstrated that the stability of the thermohaline circulation is closely linked to the surface freshwater flux (e.g., Rahmstorf, 1996). Though differences between our two experiments are weak, the response of the model thermohaline circulation to a freshwater perturbation might depend on the formulation used in order to represent the surface freshwater inflow/outflow. To our knowledge, the stability of the thermohaline circulation has never been tested using the realistic freshwater flux approach. Such a study should be carried out in order to confirm or infirm previous research results. Furthermore, the response of the ocean and climate to massive freshwater inflow, such as the discharge of more than 10^{14} m^3 of freshwater in the North Atlantic 8200 years ago (Barber et al., 1999), should also be investigated using this new formulation.

Acknowledgements

T. Fichefet and H. Goosse are Research Associate and Senior Research Assistant at the National Fund for Scientific Research (Belgium), respectively. This study was done within the scope of the Global Change and Sustainable Development Programme (Belgian State, Prime Minister's Services, Federal Office for Scientific, Technical, and Cultural Affairs, Contract CG/DD/09A) and the Concerted Research Action 097/02-208 (French Community of Belgium, Department of

Education, Research, and Formation). All of this support is gratefully acknowledged. The comments from the two anonymous referees helped to improve the paper.

References

Barber, D.C., Dyke, A., Hillaire-Marcel, C., Jennings, A.E., Andrews, J.T., Kerwin, M.W., Bilodeau, G., McNeely, R., Southon, J., Morehead, M.D., Gagnon, J.-M., 1999. Forcing of the cold event of 8200 years ago by catastrophic drainage of Laurentide lakes. Nature 400, 344–348.

Bard, E., Hamelin, B., Arnold, M., Montaggioni, L., Cabioch, G., Faure, G., Rougerie, F., 1996. Deglacial sea-level record from Tahiti corals and the timing of global meltwater discharge. Nature 382, 241–244.

Baumgartner, A., Reichel, E., 1975. The World Water Balance. Elsevier, Amsterdam, p. 179.

Beron-Vera, F.J., Ochoa, J., Ripa, P., 1999. A note on the boundary conditions for salt and freshwater balances. Ocean Modelling 1, 111–118.

Bond, G., Heinrich, H., Broecker, W.S., Labeyrie, L., McManus, J., Andrews, J., Huon, S., Jantschik, R., Clasen, S., Simet, C., Tedesco, K., Klas, M., Bonani, G., Ivy, S., 1992. Evidence for massive discharges of icebergs into the north atlantic ocean during the last glacial period. Nature 360, 245–249.

Broecker, W.S., Peng, T.-H., Jouzel, J., Russell, G., 1990. The magnitude of global fresh-water transports of importance for ocean circulation. Climate Dynamics 4, 73–79.

Bryan, K., 1969. A numerical method for the study of the circulation of the world ocean. Journal of Computational Physics 4, 347–376.

Cai, W., 1996. The stability of NADWF under mixed boundary conditions with an improved diagnosed freshwater flux. Journal of Physical Oceanography 26, 1081–1087.

da Silva, A.M., Young, C.C., Levitus, S., 1994. Atlas of the Surface Marine Data 1994. vol. 1, Algorithms and Procedures. US Dept. of Commerce. NOAA Atlas NESIDS 6, Washington, DC, p. 83.

England, M.H., 1995. Using chloroflurocarbons to assess ocean climate models. Geophysical Research Letters 22, 3051–3054.

Fichefet, T., Morales Maqueda, M.A., 1997. Sensitivity of a global sea ice model to the treatment of ice thermodynamics and dynamics. Journal of Geophysical Research 102 (C6), 12609–12646.

Gent, P.R., Bryan, F.O., Danabasoglu, G., Doney, S.C., Holland, W.R., Large, W.G., McWilliams, J.C., 1998. The NCAR climate system model global ocean component. Journal of Climate 11, 1287–1306.

Goosse, H., Campin, J.-M., Fichefet, T., Deleersnijder, E., 1997. Impact of sea-ice formation on the properties of Antarctic bottom water. Annals of Glaciology 25, 276–281.

Goosse, H., Deleersnijder, E., Fichefet, T., England, M.H., 1999. Sensitivity of a world ocean model including sea ice and CFC transport to the parametrization of vertical mixing. Journal of Geophysical Research 104 (C6), 13681–13695.

Grabs, W., De Couet, T., Pauler, J., 1996. Freshwater fluxes from continents into the world oceans based on data of the global runoff data base. Global Runoff Data Centre Report, vol. 10, Federal Institute of Hydrology, Koblenz, Germany, p. 228.

Huang, R.X., 1993. Real freshwater flux as a natural boundary condition for the salinity balance and thermohaline circulation forced by evaporation and precipitation. Journal of Physical Oceanography 23, 2428–2446.

Kwok, R., Rothrock, D.A., 1999. Variability of fram strait ice flux and North Atlantic oscillation. Journal of Geophysical Research 104 (C3), 5177–5189.

Levitus, S., 1982. Climatological atlas of the world ocean. NOAA Professional Paper, vol. 13, US Government Printing Office, Washington, DC, p. 173.

Manabe, S., Stouffer, R.J., 1995. Simulation of abrupt climate change induced by freshwater input to the North Atlantic Ocean. Nature 378, 165–167.

McDonald, A., 1993. Property fluxes at 30°S and their implications for the Pacific-Indian throughlfow and the global heat budget. Journal of Geophysical Research 98 (C4), 6851–6868.

McDonald, A., Wunsch, C., 1996. An estimate of global ocean circulation and heat fluxes. Nature 382, 436–439.

Rahmstorf, S., 1996. On the freshwater forcing and transport of the Atlantic thermohaline circulation. Climate Dynamics 12, 799–811.

Roullet, G., Madec, G., 2000. Salt conservation, free surface and varying levels: a new formulation for ocean general circulation models. Journal of Geophysical Research 105 (C10), 23927–23942.

Stocker, T.F., Schmittner, A., 1997. Influence of CO_2 emission rates on the stability of the thermohaline circulation. Nature 388, 862–865.

Stommel, H., 1984. The delicate interplay between wind-stress and buoyancy input in ocean circulation: the Goldsbrough variations. Tellus 36A, 111–119.

Wadley, M.R., Bigg, G.R., Stevens, D.P., Johnson, J.A., 1996. Sensitivity of the North Atlantic to surface forcing in an ocean general circulation model. Journal of Physical Oceanography 26, 1129–1141.

Webster, P.J., 1994. The role of hydrological processes in ocean–atmosphere interactions. Reviews of Geophysics 32, 427–476.

Wijffels, S.E., Schmitt, R.W., Bryden, H.L., Stigebrandt, A., 1992. Transport of freshwater by the oceans. Journal of Physical Oceanography 22, 155–162.

Xie, P., Arkin, P.A., 1996. Analyses of global monthly precipitation using gauge observations, satellite estimates and numerical model predictions. Journal of Climate 9, 840–858.